Architecture of North Atlantic contourite drifts modified by transient circulation of the Icelandic mantle plume

Parnell-Turner, Ross; White, Nicholas; McCave, I. Nick; Henstock, Timothy J.; Murton, Bramley; Jones, Stephen

DOI:
10.1002/2015GC005947

Supplementary Information for "Architecture of North Atlantic Contourite Drifts Modified by Transient Circulation of the Icelandic Mantle Plume"

Ross Parnell-Turner[1,4], Nicky White[1], I. Nick McCave[1], Tim Henstock[2], Bramley Murton[2], Stephen M. Jones[3]

Corresponding authors: R. Parnell-Turner and N. White, Bullard Laboratories, Department of Earth Sciences, University of Cambridge, Madingley Road, Cambridge, CB3 0EZ, UK. (rparnellturner@whoi.edu, njw10@cam.ac.uk)

[1]Department of Earth Sciences, University of Cambridge, Cambridge, CB3 0EZ, UK

[2]National Oceanography Centre Southampton, University of Southampton, European Way, Southampton SO14 3ZH

[3]School of Geography, Earth and Environmental Sciences, University of Birmingham, B15 2TT, UK

[4]Now at: Woods Hole Oceanographic Institution, Woods Hole, MA, USA

Contents of this file

1. Description of seismic reflection profiles

2. Description of Hatton Drift

3. Compaction parameter analysis

4. Figures:

– Figure S1: Seismic profiles 1 and 2

– Figure S2: Portion of profile 2 from Hatton Drift

– Figure S3: Portion of profile 1 from Eirik Drift

– Figure S4: Portion of profile 1b from Eirik Drift

– Figure S5: Detailed seismic images from Gardar drift

– Figure S6: Compaction parameter estimates from well-log data

1. Seismic reflection profiles

In this supplementary material, we present complete versions of seismic reflection profiles 1 and 2 (Figure S1). These profiles show the gross distribution and thickness of sedimentary drifts in the Iceland and Irminger Basins (e.g. Björn, Gardar, Eirik and Hatton Drifts). Figure S2 shows the detailed architecture of Hatton Drift imaged on profile 2. Figure S3 shows the westernmost portion of profile 1, where a section of Eirik Drift is imaged. Figure S4 shows Eirik Drift imaged along profile 1b, which connects profiles 1 and 2 along the Greenland continental margin. Figure S5 shows detailed portions of seismic images over Gardar Drift from profiles 1 and 2.

2. Hatton Drift

Hatton Drift sits on the lower slope of Hatton Bank which is located on the north-west side of Rockall Plateau (Figures 1, S1 and S2). Maury Channel separates Hatton and Gardar Drifts. Turbidity currents periodically transport volcaniclastic sediments through this channel southward from Iceland [*Ruddiman*, 1972]. Sediments from Hatton Drift have been recovered at various DSDP/ODP drilling sites (e.g. 403, 404, 552, 553, 555; Figure 1b). These sediments consist of carbonate oozes with occasional interbedded terrigenous material within the upper few tens of meters [*Stow and Holbrook*, 1984]. Sediments recovered in piston core V27-111 have an average silt-plus-sand content of 35% increasing to $\sim$ 70% toward the top. The carbonate-free coarse fraction is arkosic (80% quartz and feldspar) and was presumably sourced from the continental shelf of the nearby Rockall Plateau at glacial low sea levels [*McCave et al.*, 1980]. Rippled sand dunes are visible on photographs and sidescan sonar images acquired during deep camera tows on Cruise KN-51 at the foot of Hatton Drift [see Figure 5 of *McCave et al.*, 1980]. The predominantly foraminiferal sand has ripple and dune structures. It originates by winnowing beneath a northward-flowing boundary current [*McCave et al.*, 1980; *McCartney*, 1992].

The oldest material recovered from Hatton Drift consists of Late Paleocene volcaniclastic and terrigenous sediments at Site 555. These deposits lie on top of igneous basement [*Stow and Holbrook*, 1984]. A widespread non-depositional event occurred through much of Eocene and Oligocene times and is visible at most Hatton Drift drilling sites. This hiatus has been attributed to a global change in bottom-water circulation, triggered by a combination of pronounced Antarctic cooling and development of strong Antarctic Bottom Water flow into the Atlantic Ocean and formation of Labrador Sea Water [*Schnitker*, 1980;

Woodruff and Savin, 1989; *Zachos et al.*, 1993]. Major growth of Hatton Drift probably commenced during mid-Miocene times, with deposition of biogenic sediments continuing into Holocene times [*Stow and Holbrook*, 1984].

Profile 2 traverses part of Hatton Drift on the northeast side of Rockall Plateau where it is $\sim$ 32 km wide (Figure S2). Drift sediments lie on the shoulder of Hatton Bank which has a basement slope of $\sim 2°$. They can be divided into four units named H-I to H-IV. The youngest unit of Hatton Drift, H-I, consists of a 60 m thick continuous series of conformable reflections (Figure S2d). This unit represents the most recent sedimentary drape deposited by modern current activity. A package characterized by disrupted reflections, H-II, lies directly underneath. This unit is up to 85 m thick and is acoustically transparent in places. The base of H-II is marked by an erosional surface that truncates the continuous reflections of H-III beneath. Unit H-II could be a debris flow or a mass-transport complex, perhaps related to sediment supplied from the upslope direction on Hatton Bank. Unit H-III is up to 230 m thick and comprises the main body of Hatton Drift on Profile 2. Continuous reflections within unit H-III are easily identified but they are often truncated by localized erosional surfaces and by minor buried channels (Figure S2b). Stratigraphic onlap occurs at the base of unit H-III which lies unconformably above H-IV, the lowest mappable unit. H-IV is probably the pre-drift sedimentary pile. Normal faulting occurs at the sediment-basement interface and occasional faults reach the sea bed. Stratigraphic growth occurs within H-IV but there is little evidence for growth within the Hatton Drift itself.

2.1. Compaction parameters

We analyzed porosity-depth relationships from Sites 646 (Eirik Drift) and 984 (Björn Drift) to determine the values of the initial porosity, $\phi_\circ$, and the compaction decay length, λ (Figure S6). These parameters were used to determine solid accumulation rates for drift deposits.

References

Schnitker, D. (1980), Global paleoceanography and its deep water linkage to the Antarctic glaciation, *Earth-Science Reviews*, *16*, 1–20.

Stow, D. A. V., and J. A. Holbrook (1984), Hatton Drift contourites, Northeast Atlantic, in *Init. Rep. Deep Sea Drill. Proj. 81*, edited by D. G. Roberts, D. Schnitker, et al., pp. 695–699, U.S. Govt. Printing Office, Washington.

Woodruff, F., and S. M. Savin (1989), Miocene deepwater oceanography, *Paleoceanography*, *4*(1), 87–140.

Zachos, J. C., K. C. Lohmann, J. C. G. Walker, and S. W. Wise (1993), Abrupt Climate Change and Transient Climates during the Paleogene: A Marine Perspective, *Journal of Geology*, *101*, 191–213.

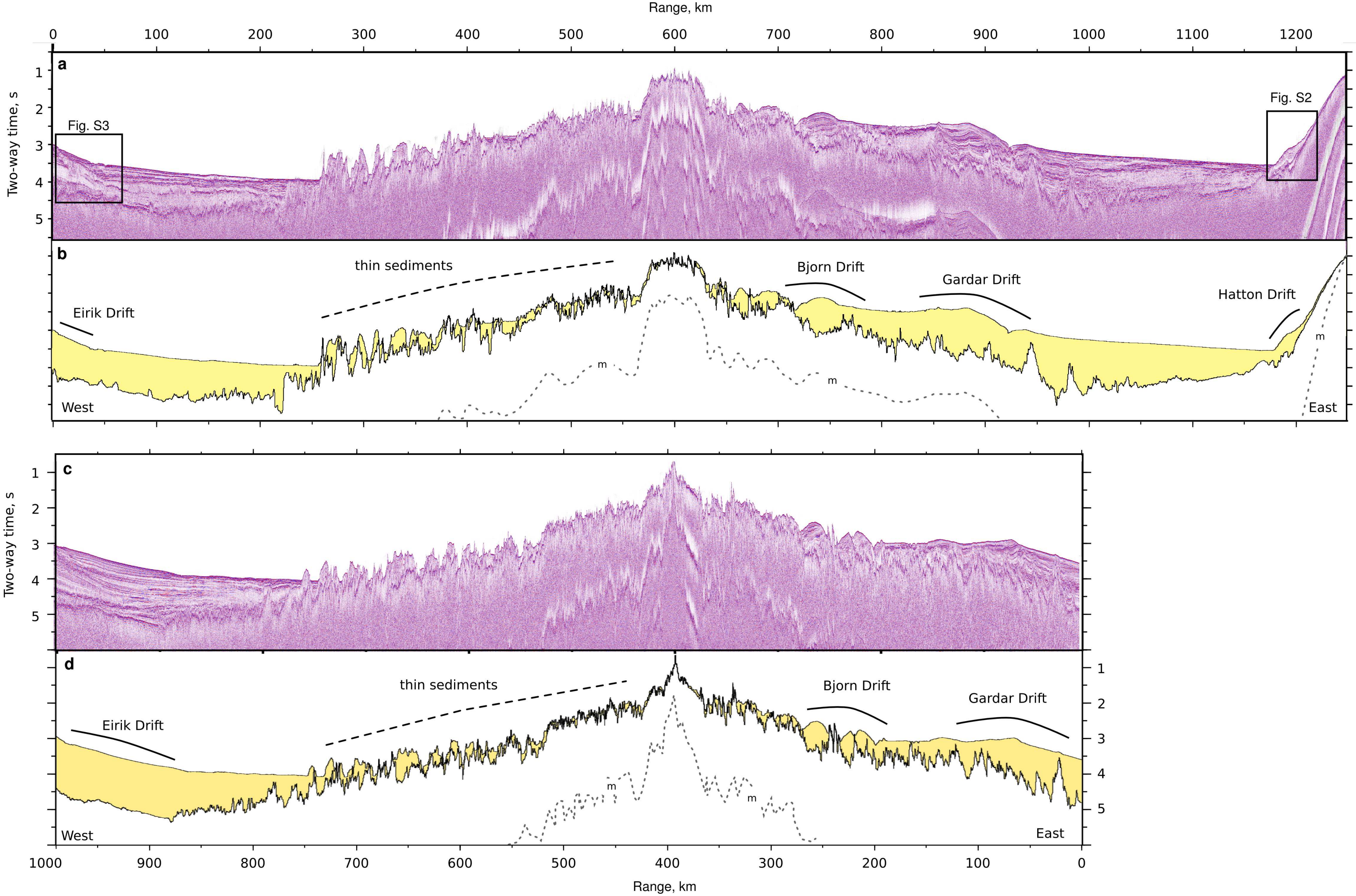

Figure S1: Time-migrated seismic reflection profiles 1 and 2 (see Figure 1 for location). a) Profile 2. Boxes show location of Figures S2 and S3. b) Interpretation. Solid lines = sedimentary drifts; yellow shading = sedimentary cover; dashed line = thin sediments; m = seabed multiple. c) Profile 1. b) Geologic interpretation. Note thin sediments are distributed along the western flank of the Reykjanes Ridge, however modern day body of Snorri Drift does not extend as far south as profile 2 (i.e. 62°N).

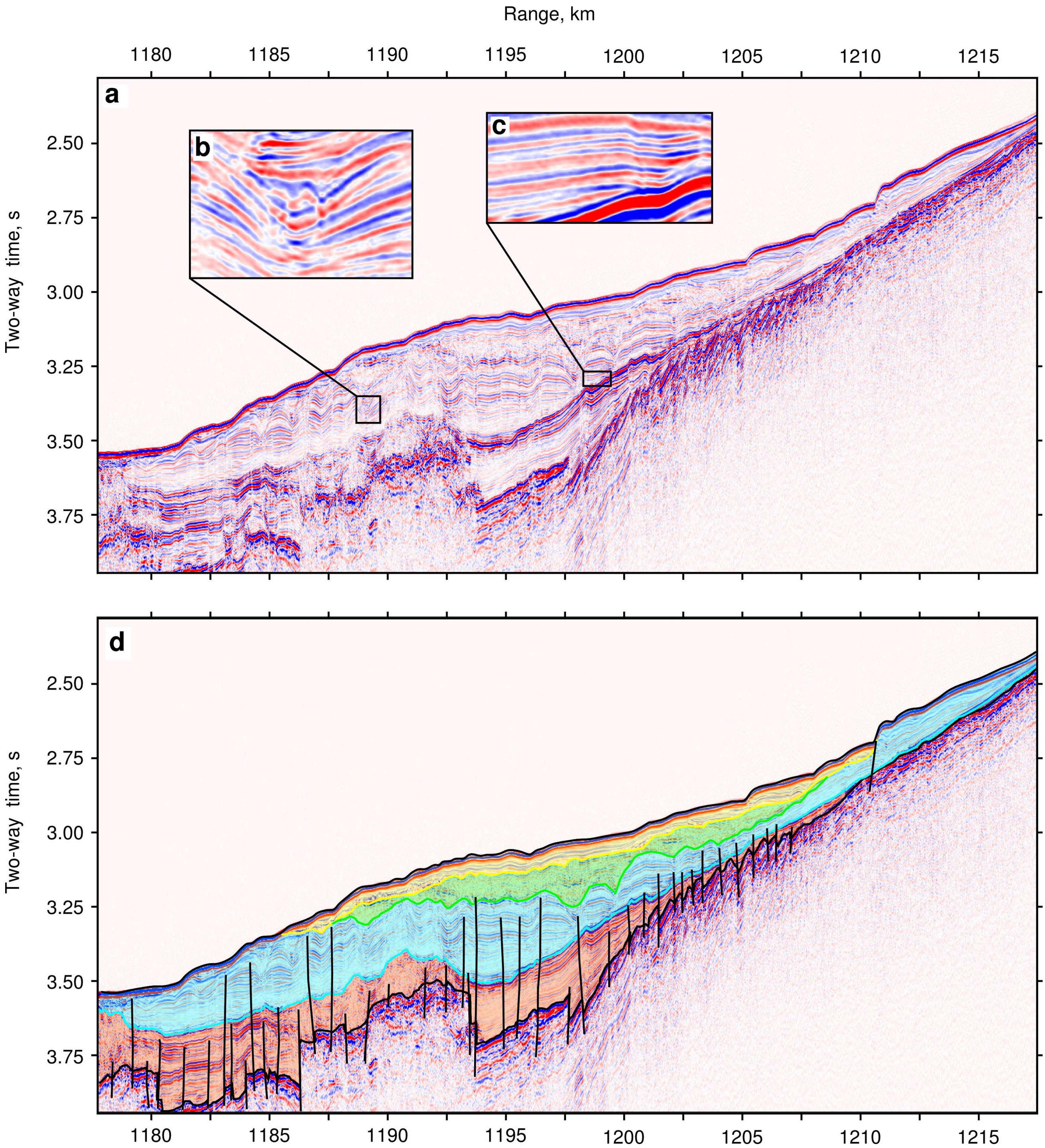

Figure S2: (a) Portion of profile 2 which crosses Hatton Drift (see Figures S1 and 1c for location). (b) and (c) Insets showing details of buried channel and onlapping stratigraphy, respectively. (d) Interpretation. Colored lines/intervals = interpreted horizons/units: yellow = H-I; green = H-II; blue = H-III; orange = H-IV; black line = basement; black lines = normal faults.

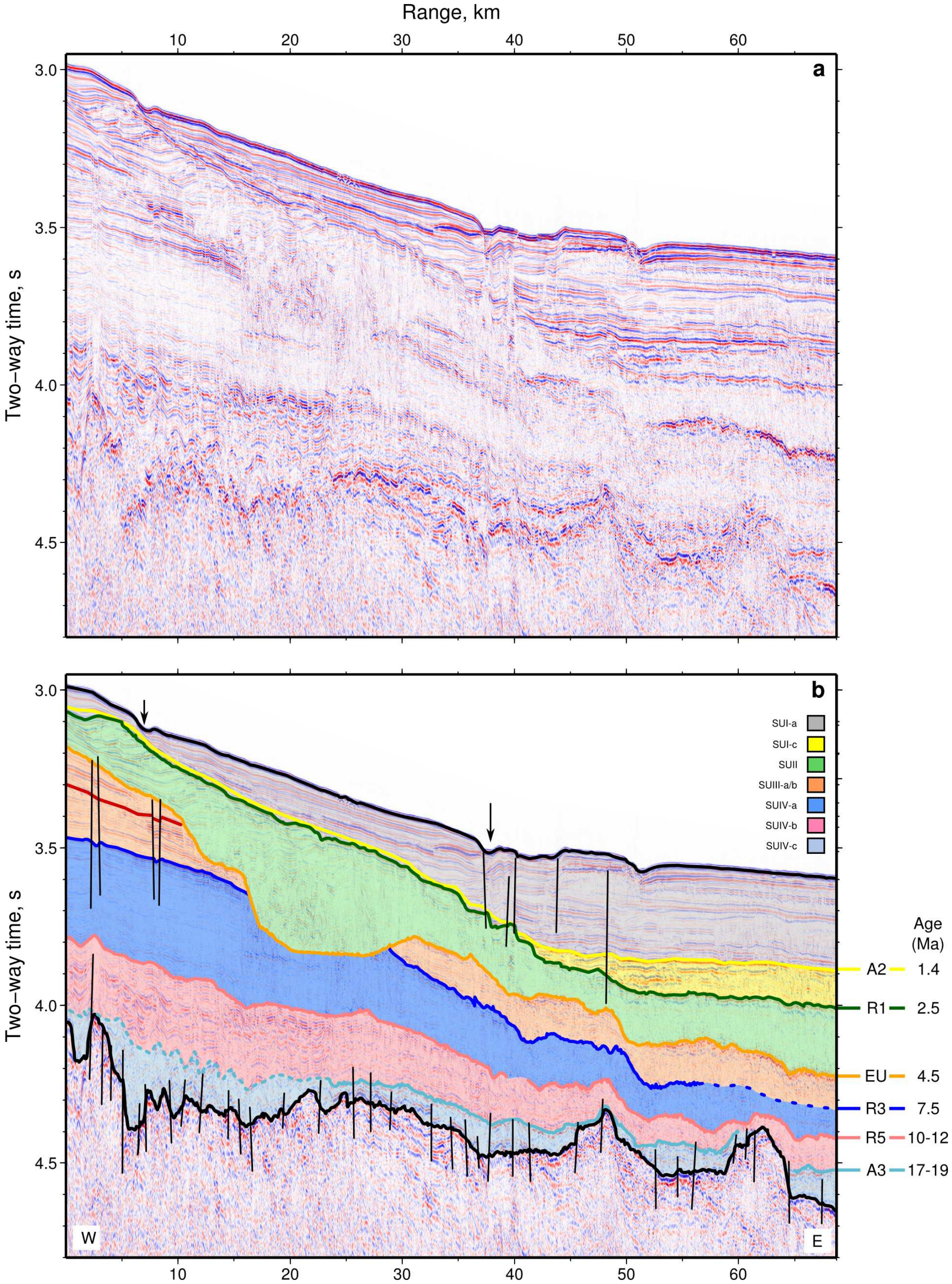

Figure S3: (a) Portion of profile 2 which crosses Eirik Drift (see Figure 1c for location). (b) Interpretation. Colored lines = interpreted horizons with ages noted; colored intervals = stratigraphic units; upper/lower black lines = seabed/basement reflections, respectively; black lines = faults; arrows = bounding channels.

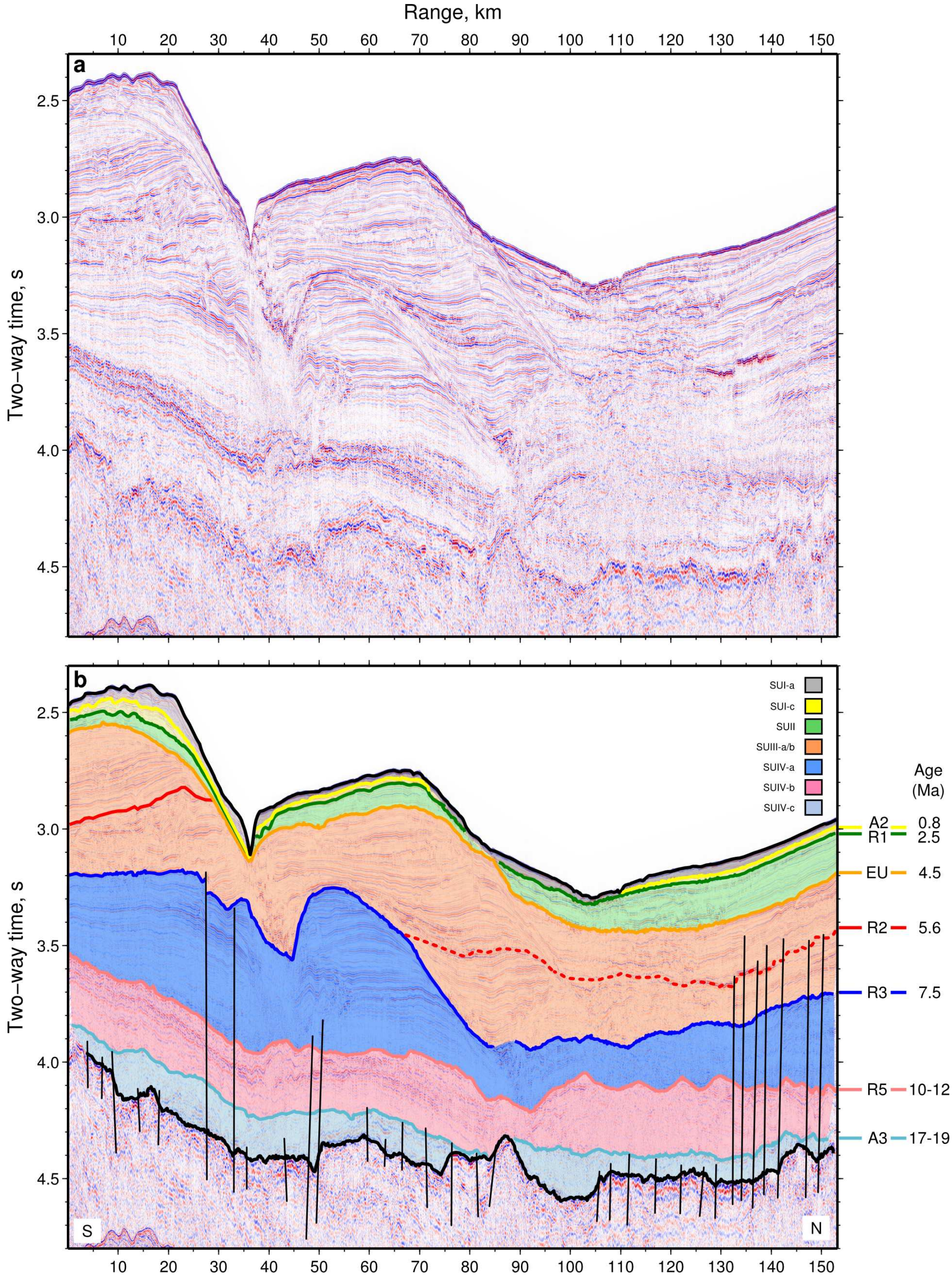

Figure S4: (a) Portion of profile 1b located parallel to Greenland margin (see Figure 1c for location). (b) Interpretation. Colored lines = dated horizons; red dotted lines = interpretation of R2; colored intervals = stratigraphic units; upper/lower black lines = seabed/ basement reflections, respectively; black lines = faults. Subset of sedimentary units from Eirik Drift are seen. Two modern channels visible at ranges of 35 and 105 km. These channels initiated at R3 time (7.5 Ma), and have since migrated ∼10 km southwards. Buried channel located at range 85 km. Channel initiated post-R5 times (10–12 Ma) and since southward by ∼15 km until R3 times (7.5 Ma).

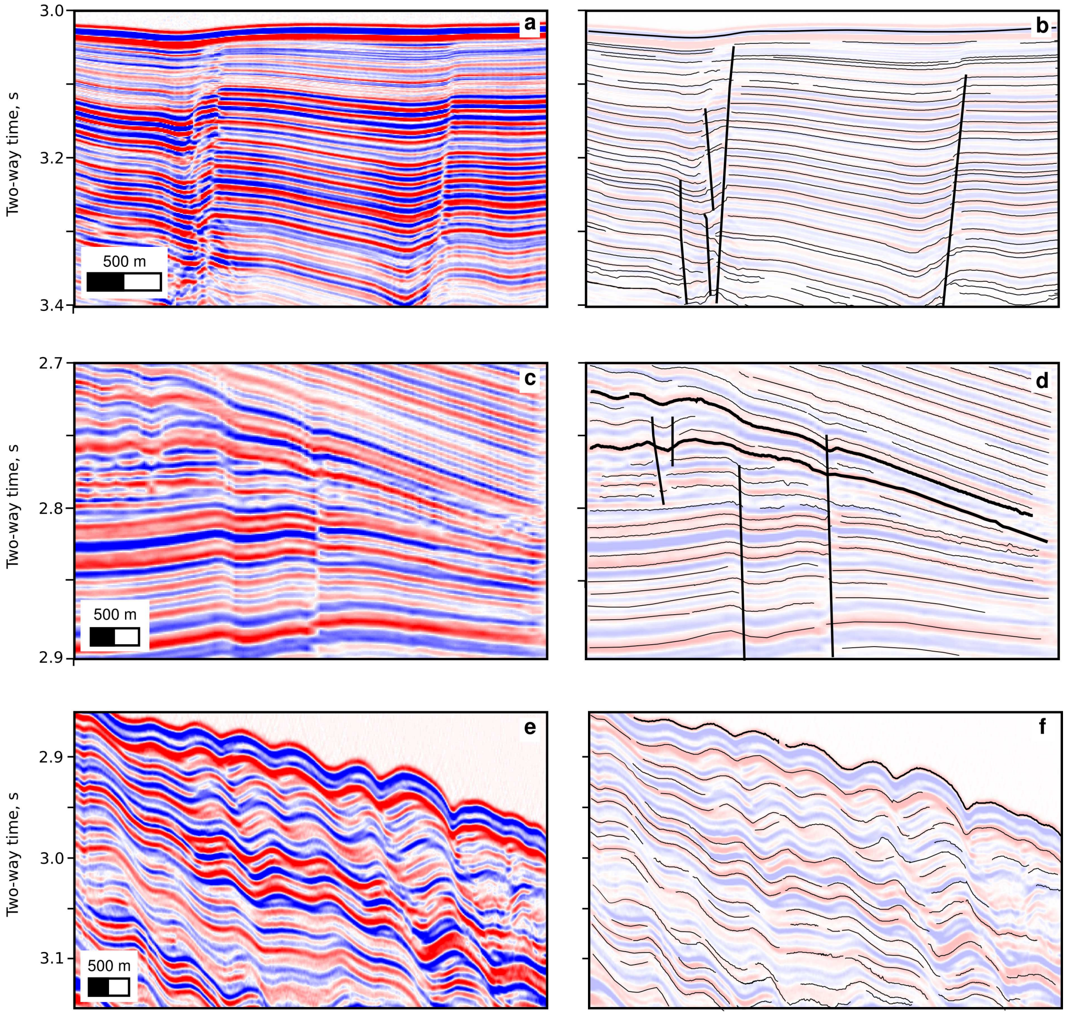

Figure S5: Detailed images of Gardar drift (see Figure 9 for location). (a) Detailed section of profile 1 at range of 80 km. (b) Interpretion showing normal faults and minor stratigraphic growth features. Thick lines = faults; thin lines = stratigraphic interpretation. (c) Detailed section of profile 2 at range of 89 km. (d) Interpretation showing two unconformity surfaces (bold lines) where older unit is truncated by overlying strata. (e) Detailed section of profile 2 at range of 920 km. (f) Interpretation showing westward-migrating mudwaves on eastern slope of drift. Mudwaves at seabed are ∼25 m in amplitude, ∼500 m in wavelength.

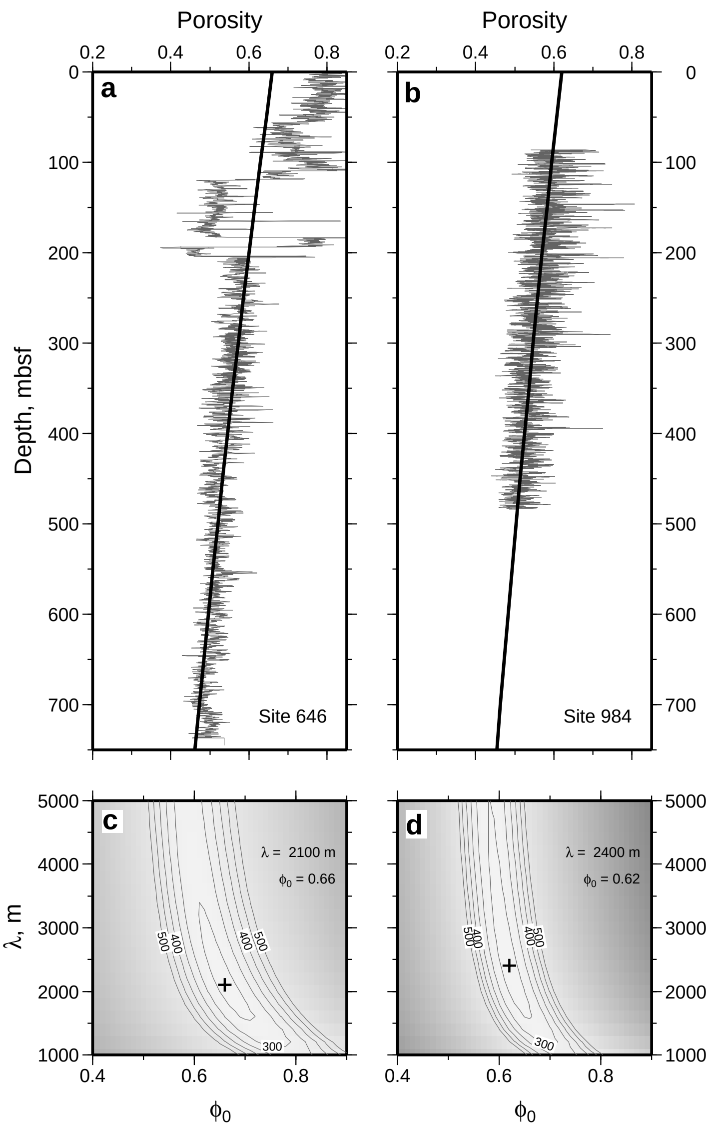

Figure S6: Porosity-depth relationship for Eirik and Björn Drifts from downhole log data. (a) Site 646 (Eirik Drift). Thin gray line = compensated neutron porosity. Noise at depths <220 m due to logging through drill pipe; black line = porosity calculated using best-fitting compaction parameters given in (c). (b) Site 984 (Björn Drift). (c) Misfit plot for compaction parameters $\phi_\circ$ and λ at Site 646. Cross = misfit minimum. (c) Misfit plot for compaction parameters $\phi_\circ$ and λ at Site 984.